

Electrically Induced Two-Photon Transparency in Semiconductor Quantum Wells

Alex Hayat, Amir Nevet, and Meir Orenstein

Department of Electrical Engineering, Technion, Haifa 32000, Israel

(Received 13 February 2009; published 5 May 2009)

We demonstrate experimentally two-photon transparency, achieved by current injection into a semiconductor quantum-well structure which exhibits two-photon emission. The two-photon induced luminescence is progressively reduced by the injected current, reaching the point of two-photon transparency—a necessary condition for semiconductor two-photon gain and lasing. These results agree with our calculations.

DOI: 10.1103/PhysRevLett.102.183002

PACS numbers: 32.80.Wr, 42.50.Hz

Two-photon processes involve second-order electron transitions between energy levels via virtual states, by absorbing or emitting photon pairs [1]. Two-photon absorption (TPA) is important in various scenarios at high field intensities [2,3], whereas two-photon emission (TPE) continuous-spectrum has significance for astrophysics [1,4], and atomic physics [5]. While semiconductor TPA has been substantially investigated and used, e.g., in coherent-control applications [6–9], TPE in semiconductors was only recently observed [10], enabling possible realizations of efficient electrically driven heralded single-photon sources, entanglement sources [11,12], two-photon amplifiers [13–15] and novel lasers allowing ultrashort optical pulse generation based on the nonlinearity and the wide bandwidth of two-photon gain. Two-photon lasers (TPL) based on stimulated TPE [16] have unique microscopic quantum properties such as squeezed state operation [17] as well as macroscopic ones including threshold dependence on cavity photon number and bistability [18]. Two-photon gain (TPG) and lasing were demonstrated only in discrete-level atomic systems by injecting atoms in a well-prepared state into a high quality cavity, yielding relatively low intensities. Semiconductor high charge carrier concentrations, mature fabrication technology, and the possibility for electrical control offer many advantages for the realization of TPLs and two-photon amplifiers [13–15]. The necessary condition towards the realization of semiconductor amplifiers or TPLs is achieving the two-photon transparency (TPT) condition, which we report here for the first time in semiconductors, to the best of our knowledge.

In this Letter we present the experimental observation of TPT and controlled TPA in an electrically driven semiconductor quantum-well (QW) structure. Because of the dependence of the two-photon transition matrix element on crystal momentum— k , even for parabolic bands [9], in bulk semiconductors most of the TPA for wideband light pulses should occur at higher- k states. Thus current-controlled TPA in bulk semiconductors requires significant carrier population at high- k (high energy) states which is more difficult to achieve. Our experiments are based rather

on a QW structure, where the nearly energy-independent electron state density for each subband allows much easier injection control and cancellation of TPA due to a larger low- k contribution. The net semiconductor TPG coefficient is [13]

$$\gamma_2 = (2\hbar\omega_p/I^2)M \quad (1)$$

where I is the light intensity, ω_p is the photon angular frequency, and M is the two-photon transition matrix element given by

$$M = \frac{2\pi}{\hbar} \left(\frac{4\pi^2 e^4 I^2}{n_p^2 c^2 m^4 \omega_p^4} \right) \sum_f \int |\mu|^2 [F_c(k) - F_v(k)] \times \delta(E_f - E_i - 2\hbar\omega_p) \frac{dk}{(2\pi)^3}, \quad (2)$$

where $F_c(k) = 1/\{\exp[E_c(k) - E_{FC}]/k_B T + 1\}$ and $F_v(k) = 1/\{\exp[E_v(k) - E_{FV}]/k_B T + 1\}$ are the quasi Fermi-Dirac distribution functions for the conduction and the valence bands, respectively, with the corresponding quasi Fermi energies E_{FC} and E_{FV} , n_p is the refractive index at ω_p , m is the electron mass, c is the vacuum light velocity, e is the electron charge, k is the crystal momentum, k_B is the Boltzmann constant, T is the absolute temperature, and indices f and i stand for the initial and final states. In Eq. (2), μ includes the summation

$$\mu = \sum_n \frac{\langle f | \vec{\varepsilon} \cdot \hat{p} | n \rangle \langle n | \vec{\varepsilon} \cdot \hat{p} | i \rangle}{E_n - E_i - \hbar\omega_p}, \quad (3)$$

where \hat{p} is the momentum operator, $\vec{\varepsilon}$ is the photon polarization, and the summation is over all the intermediate states n . When the current injection dependent quasi Fermi energy separation $\Delta E_F = E_{FC} - E_{FV}$ satisfies the condition $\Delta E_F > 2\hbar\omega_p$ the TPG coefficient γ_2 becomes positive [Fig. 1(a)], while at lower carrier injection the gain is negative, corresponding to two-photon absorption.

The direct probing of TPG in QW is obstructed by a competing effect of free-carrier absorption (FCA) [Fig. 1(c)] occurring in the entire photonic volume of the device determined by the waveguide mode volume, in

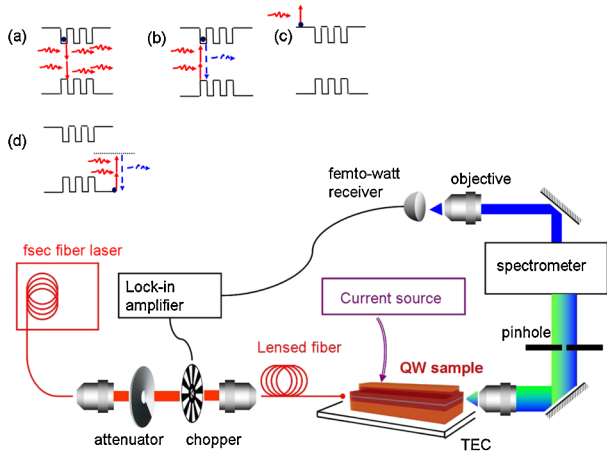


FIG. 1 (color online). Electrically controlled TPA-luminescence measurement setup. The insets are the diagrams of different processes: (a) TPG, (b) TPA-luminescence, (c) FCA, (d) SHG.

contrast to TPG and TPA that are confined to the QWs (the lowest bandgap material of the structure). In order to isolate the two-photon effects, we monitored the TPA-induced carrier population by measuring the induced one-photon emission from the QWs—namely, TPA luminescence [Fig. 1(b)]. The TPA-induced carrier concentration is given by $n_e = -\Gamma\gamma_2 I^2 \tau_e / \hbar\omega_p$, where τ_e is the carrier lifetime, and Γ is the confinement factor. For a small injection current, the negative values of γ_2 appear as a positive difference in carrier concentration causing TPA-induced luminescence, while at a specific higher current quasi Fermi level separation causes γ_2 to vanish [Eq. (2)] making the QWs two-photon transparent resulting in the cancellation of TPA luminescence.

In our experiments, we first monitored the spontaneous TPE from a 4 μm wide, 1500 μm long ridge waveguide with an embedded structure of three 8 nm $\text{Al}_{0.14}\text{Ga}_{0.84}\text{As}$ QWs separated by 10 nm $\text{Al}_{0.3}\text{Ga}_{0.7}\text{As}$ barriers grown on GaAs. The TPE was measured filtering out of the wideband TPE a specific wavelength range of 1545–1555 nm related to the input pulse spectrum in the subsequent measurements, by methods reported in [10] for a different QW structure. The intensity of the TPE (after filtering any residual one-photon emission by a thick Si layer) has a linear dependence on the injection current level (Fig. 3 inset) and the collected power was on the order of 1 pW.

TPA-induced luminescence measurements were performed using a mode-locked fiber laser source (OptiSiv) generating ~ 100 fs pulses at 1560 nm central wavelength, 30 MHz repetition rate and 40 mW mean power, facet-coupled by a lensed fiber (Fig. 1) into the waveguide. The QW photoluminescence exhibits peak emission near 770 nm. In order to isolate TPA-induced luminescence from current-induced electroluminescence, the femtosecond laser pulse train was modulated at 513 Hz. The mean input power coupled to the waveguide was tuned using a

free-space attenuator, while overall measured 40 dB waveguide insertion loss was included. A thermoelectric cooler was set to 294° K throughout the measurements. The current injection into the QW structure was controlled, maintaining it well below the single-photon lasing threshold. The electrically controlled TPA-induced luminescence was measured by a “femtowatt” receiver, connected to a lock-in amplifier locked on the 513 Hz modulation of the input laser. The effect of FCA was calibrated by measuring the current-induced absorption of a continuous-wave 1560 nm laser (Fig. 2 inset) using an infrared detector. Second harmonic generation (SHG) [Fig. 1(d)], which is a competing effect due to a significant second-order non-linearity in such materials [19–21], has parabolic input intensity dependence similarly to TPA; however, SHG is not current dependent and is centered at half the input wavelength, and thus can be easily distinguished from the resonant TPA luminescence centered at shorter wavelengths and depending on carrier distribution.

The measured spectra (Fig. 2) exhibit TPA-induced luminescence, current-induced electroluminescence and SHG. Electroluminescence, measured with no input laser, is centered at ~ 760 nm matching the calculations including bandgap shrinkage effect [22] and Auger recombination [23]. For carrier concentration of $\sim 5 \times 10^{17} \text{ cm}^{-3}$ generated by current injection, the TPA-induced luminescence is centered at ~ 750 nm in accordance with the calculations. On the other hand, the SHG is centered at ~ 780 nm—at half of the femtosecond laser central wavelength, having a spectral line shape similar to that of the input laser vs half the wavelength, as expected. The TPA luminescence is modulated by the input power modulation and therefore the carrier concentration added by the TPA can be easily distinguished from that generated by the

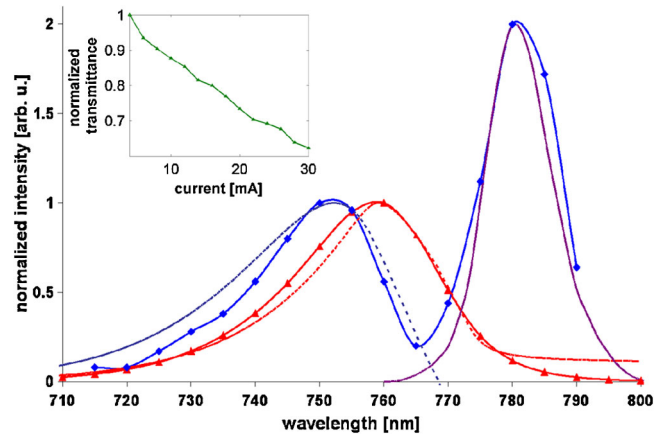


FIG. 2 (color online). Spectra measurements with $\sim 5 \times 10^{17} \text{ cm}^{-3}$ current-induced carrier injection. The red triangles are the measured spectrum of the electroluminescence alone, and the red dashed line is the calculated spectrum. Blue squares are both TPA luminescence and SHG. The dashed blue line is the calculated TPA-luminescence spectrum and the purple solid line—measured femtosecond laser spectrum plotted vs half the wavelength. The inset is the FCA vs current injection.

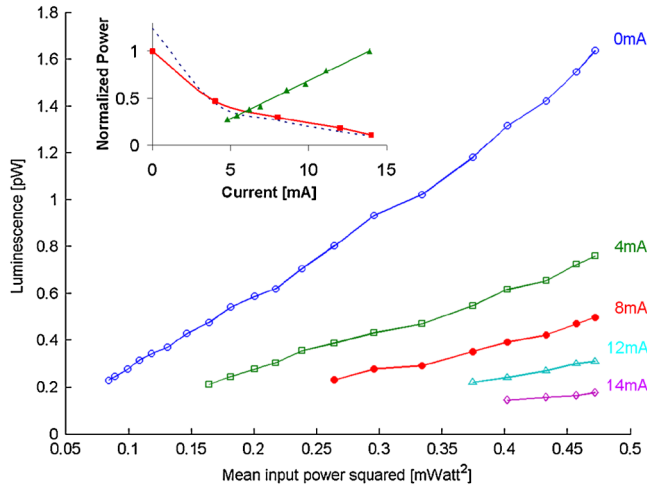


FIG. 3 (color online). Measured electrically controlled TPA luminescence vs input power squared at various currents. No current (blue circles), 4 mA (green squares), 8 mA (red filled circles), 12 mA (cyan triangles), and 14 mA (purple diamonds). The inset is the injection current dependence of TPA luminescence at $\sim 650 \mu\text{W}$ input: measured (red filled squares) and calculated (blue dashed line); and spontaneous TPE (green triangles).

current injection. Moreover, the TPA-induced carrier concentration is added to the existing current-induced concentration resulting in higher energy populated states and thus the corresponding emission is shifted towards shorter wavelengths relative to the electroluminescence (Fig. 2).

The current dependence of the TPA luminescence is calculated considering the measured power coupled into the waveguide and the γ_2 coefficient of similar QW structures [24]. The resulting value of TPA-induced carrier supplement is calculated to be $\sim 1.25 \times 10^{16} \text{ cm}^{-3}$ with the corresponding luminescence energy distribution in good agreement with experimental results (Fig. 2).

The dependence of the TPA-induced luminescence on input power was measured at various current injection levels after taking into account the effect of SHG and FCA (Fig. 3). The input power dependence is quadratic as expected and is progressively suppressed by the current injection, which makes the TPG coefficient γ_2 less negative. The luminescence current dependence clearly shows the reduction of $|\gamma_2|$ with injection conforming to our theoretical results (Fig. 3 inset). In our specific device the TPA vanishes at an injection current of $\sim 16 \text{ mA}$ ($\sim 100 \text{ A/cm}^2$ current density), reaching the TPT point. Injection current higher than 16 mA results in positive γ_2 value, namely, QW TPG, however the related higher carrier concentration also increases the FCA and thus results in net insertion loss in this experiment, due to the relatively weak two-photon process. The nonlinear TPG can overcome the FCA process only for intense input pulses efficiently coupled into the waveguide, which requires specially designed photonic structures, with high confinement factors and improved coupling.

In conclusion, we have demonstrated experimentally TPT and controlled TPA in electrically driven semiconductor QWs, which to the best of our knowledge, have not been demonstrated before. After eliminating the contributions of FCA and SHG, the observed TPA-induced luminescence has quadratic dependence on the input power. The TPA was shown to be reduced by the injected current and to reach the TPT condition. In the specific QW structure employed in our experiments the TPT is achieved at $\sim 16 \text{ mA}$ injection current. The demonstration of electrically induced two-photon transparency is a necessary step towards the implementation of future semiconductor two-photon lasers.

- [1] J. Chluba and R. A. Sunyaev, *Astron. Astrophys.* **446**, 39 (2006).
- [2] V. Nathan, A. H. Guenther, and S. S. Mitra, *J. Opt. Soc. Am. B* **2**, 294 (1985).
- [3] C. C. Lee and H. Y. Fan, *Phys. Rev. B* **9**, 3502 (1974).
- [4] J. Shapiro and G. Breit, *Phys. Rev.* **113**, 179 (1959).
- [5] S. P. Goldman and G. W. F. Drake, *Phys. Rev. A* **24**, 183 (1981).
- [6] R. Atanasov, A. Hache, J. L. P. Hughes, H. M. van Driel, and J. E. Sipe, *Phys. Rev. Lett.* **76**, 1703 (1996).
- [7] J. B. Khurgin, *Appl. Phys. Lett.* **74**, 4 (1999).
- [8] A. Hache, Y. Kostoulas, R. Atanasov, J. L. P. Hughes, J. E. Sipe, and H. M. van Driel, *Phys. Rev. Lett.* **78**, 306 (1997).
- [9] L. Costa, M. Betz, M. Spasenović, A. D. Bristow, and H. M. van Driel, *Nature Phys.* **3**, 632 (2007).
- [10] A. Hayat, P. Ginzburg, and M. Orenstein, *Nat. Photon.* **2**, 238 (2008).
- [11] A. Hayat, P. Ginzburg, and M. Orenstein, *Phys. Rev. B* **76**, 035339 (2007).
- [12] A. Hayat, P. Ginzburg, D. Neiman, S. Rosenblum, and M. Orenstein, *Opt. Lett.* **33**, 1168 (2008).
- [13] C. N. Ironside, *IEEE J. Quantum Electron.* **28**, 842 (1992).
- [14] N. Kaminski, A. Hayat, P. Ginzburg, and M. Orenstein, *IEEE Photonics Technol. Lett.* **21**, 173 (2009); C. Z. Ning, *Phys. Rev. Lett.* **93**, 187403 (2004).
- [15] D. H. Marti, M.-A. Dupertuis, and B. Deveaud, *IEEE J. Quantum Electron.* **39**, 1066 (2003).
- [16] A. M. Prokhorov, *Science* **149**, 828 (1965).
- [17] H. P. Yuen, *Phys. Rev. A* **13**, 2226 (1976).
- [18] D. J. Gauthier, Q. Wu, S. E. Morin, and T. W. Mossberg, *Phys. Rev. Lett.* **68**, 464 (1992).
- [19] S. Ducci, L. Lanco, V. Berger, A. De Rossi, V. Ortiz, and M. Calligaro, *Appl. Phys. Lett.* **84**, 2974 (2004).
- [20] L. Lanco, S. Ducci, J.-P. Likforman, X. Marcadet, J. A. W. van Houwelingen, H. Zbinden, G. Leo, and V. Berger, *Phys. Rev. Lett.* **97**, 173901 (2006).
- [21] A. Fiore, E. Rosencher, B. Vinter, D. Weill, and V. Berger, *Phys. Rev. B* **51**, 13 192 (1995).
- [22] A. Tomita and A. Suzuki, *IEEE J. Quantum Electron.* **23**, 1155 (1987).
- [23] M. Takeshima, *J. Appl. Phys.* **58**, 3846 (1985).
- [24] S. J. Wagner, J. Meier, A. S. Helmy, J. S. Aitchison, M. Sorel, and D. C. Hutchings, *J. Opt. Soc. Am. B* **24**, 1557 (2007).